The Active Layer of the Upper Atlantic Ocean

HUUG M. VAN DEN DOOL

Department of Meteorology, University of Maryland, College Park, Maryland

PETER J. LAMB* AND RANDY A. PEPPLER

Climate and Meteorology Section, Illinois State Water Survey, Champaign, Illinois

(Manuscript received 10 December 1987, in final form 23 May 1988)

ABSTRACT

The procedure to calculate the active layer depth of the upper ocean, as proposed by Van den Dool and Horel (DH), was applied to the Atlantic Ocean from 20°S to 70°N. In this method, the observed climatological annual cycle in SST is employed to invert a simple linear energy balance. The results for the Atlantic are similar to those for the Pacific Ocean in several ways. The active layer is considerably shallower than the annual mean mixed layer (which is calculated from in situ sea temperature profiles). Just as for the Pacific, however, the patterns of active and mixed layer depth show a remarkable spatial match.

Using Bunker's datasets for SST and heat transfer over the Atlantic Ocean, the forcing used in the energy balance equation was made increasingly more realistic, from (i) astronomical solar radiation, through (ii) empirical estimates of absorbed solar radiation including the modifying effect of clouds to (iii) the complete empirically determined net ocean surface heat gain. No matter what forcing was used, the calculated active layer is always much shallower than the mixed layer depth. The best pattern match was found using the simplest forcing of all—the astronomical solar forcing.

Increasingly, atmospheric models are being coupled to an oceanic slab in which the SST evolves in response to local heat gains and losses. The key question is how deep that slab should be. Our study implies that, in order to match the observed annual cycle in SST, the oceanic slab should be quite shallow, and certainly shallower than the mixed layer depth. The shallowness of the active layer implies that ocean heat transport contributes to the forcing of the annual cycle in SST in the midlatitudes of the Atlantic Ocean.

1. Introduction

The need for interactive atmosphere–ocean models for climate studies is beyond doubt. From a narrow atmospheric point of view, the only oceanic parameter that matters is the sea surface temperature (SST). The simplest way to calculate SST is to couple an atmospheric model to an oceanic slab that changes its temperature in response to the net vertical energy flux across the ocean–atmosphere interface (Manabe and Stouffer 1980; Meehl and Washington 1985; Wilson and Mitchell 1987). The key question is how thick that oceanic slab has to be to produce realistic SST. The most natural choice is the depth of the mixed layer (h_m), which is usually defined from local oceanographic temperature soundings as the near-isothermal surface layer. However, an isothermal layer is not necessarily the same as a mixed layer and the criterion for a layer being isothermal is somewhat arbitrary (e.g., Bathen 1972; Lamb 1984; and references quoted therein). Therefore a good deal of engineering is necessary to find the appropriate depth.

In an earlier paper, Van den Dool and Horel (1984, hereafter referred to as DH) described a simple method to derive the thermal inertia of the upper ocean thought to be relevant to air–sea interaction at the annual time scale. This was done by assuming that the annual course of SST can, to a first-order approximation, be described by a simple energy-balance equation. One can then estimate the heat capacity of the "active" layer of the upper ocean from the observed climatological annual variations in SST and in absorbed solar radiation. Also, one can derive how fast SST is damped towards its equilibrium value. Van den Dool and Horell found the spatial pattern of the active layer depth (h) in the North Pacific Ocean to be rather similar to that of the observed annual mean mixed layer depth. However, the active layer turned out to be only half as deep as mixed layer depths reported by Bathen (1972).

In reality the annual cycle in sea temperature decreases with depth (z) and fades away beyond $z = 500$ m (Levitus 1984). If a truly mixed layer of constant depth existed the annual cycle would be the same at

* Also affiliated with Department of Atmospheric Sciences, The University of Illinois.

Corresponding author address: Dr. Huug van den Dool, Dept. of Meteorology, University of Maryland, College Park, MD 20742.

all depths within that layer, and zero at greater depths. Since this is not the case a hypothetical layer has to be constructed that collapses the annual cycle (as it is observed from $z = \infty$ to $z = 0$) into a single perfectly mixed slab: the *active layer*. While DH employ an energy balance to find the active layer depth, alternative approaches operating on in situ temperature profiles have been used by Manabe and Stouffer (1980) and Meehl (1984). Although these approaches differ in detail, they all make recourse to the most powerful and well documented climatic variation of which we are aware—the annual cycle. Yet another method for coupling the atmosphere to the ocean has been proposed by Wilson and Mitchell (1987). They fix h_m to be 50 m, and then calculate the ocean's heat transport as a residual. This residual is, from then on, prescribed in perturbed (doubled CO_2, 9000 BC solar radiation) climates.

In this paper we will

(i) repeat DH, but for the Atlantic Ocean from 20°S to 70°N. As we shall see, the results for both oceans are very similar. Then some extensions will be made to further understand the puzzling difference between the depth of the active and the mixed layer.

(ii) Instead of an astronomical estimate of the solar radiation input to the ocean surface we will use an empirical estimate that takes into account the attenuation by clouds; in DH and under (i) the albedo and atmospheric transmission are assumed constant in space and time.

(iii) Because solar radiation may not be the only forcing of the annual cycle in SST we will also use the net surface oceanic heat gain as the forcing.

This more complete analysis of the Atlantic is possible because datasets regarding SST, mixed layer depth, and net surface heat gain have been developed from the substantial data compilations and heat exchange calculations of A. F. Bunker and the second author of this paper (Lamb and Bunker 1982; Lamb 1984; and references therein).

Extensions (ii) and (iii) may not necessarily be successful, though. Although DH's assumption that atmospheric transmission and albedo are constant in space and time is clearly incorrect, an empirical formula that takes cloudiness into account may not be accurate. The amount of solar radiation arriving at the ocean surface has rarely been measured for more than a few weeks at more than a few points. Therefore, the empirical formulae for absorbed solar radiation are often extrapolations from expressions valid in continental and coastal areas and may be seriously in error (Simpson and Paulson 1979; Dobson and Smith 1988). The situation is probably even worse for the empirical estimates that, together, define the net surface heat gain. In addition to absorbed solar radiation, the annual cycle in net surface heat gain by the Atlantic Ocean is primarily determined by evaporation from the ocean (Hastenrath and Lamb 1978). So by comparing (i) with (ii) and (iii) one also gets an impression of the overall usefulness of empirical estimates of climatological fluxes of energy at the ocean–atmosphere interface.

2. Analysis

The oceanic heat budget equation can be written

$$\rho c_p \int_0^D \frac{\partial T}{\partial t}\, dz = \mathrm{SW}\uparrow\downarrow - \mathrm{LW}\uparrow\downarrow - \mathrm{SH} - \mathrm{LE} + \mathrm{OTR}$$

$$= F\downarrow\uparrow + \mathrm{OTR} \qquad (1)$$

where t is time, c_p is specific heat, ρ is density, T is temperature, D is the depth at which T is constant in time, SW and LW are shortwave and longwave radiation fluxes, SH and LE are the sensible and latent heat fluxes, and OTR is the convergence by ocean heat transport. Heat transfer associated with falling precipitation is assumed negligible. Equation (1) states that heat storage (left hand) should equal the net in-flux of heat (right hand). All interface fluxes can be combined into $F\downarrow\uparrow$, the quantity referred to as the "net surface oceanic heat gain" in Lamb and Bunker (1982). Generally speaking, $\mathrm{LW}\uparrow\downarrow$, SH and LE represent processes by which the ocean loses heat, while $\mathrm{SW}\downarrow\uparrow$ provides the heating. The role of ocean transport and upwelling is location dependent and rarely known from direct observation. Bryan and Schroeder (1960), Lamb and Bunker (1982) and Hastenrath and Merle (1986) calculated OTR as a residual from (1) for the Atlantic. Because some of the fluxes entering $F\downarrow\uparrow$ are large, not accurately known, and tend to cancel each other, the residual OTR is usually regarded as being rather uncertain.

The annual cycle in SST is clearly caused by $\mathrm{SW}\downarrow$. Under the assumption that "everything else" just modifies and damps the response to the basic $\mathrm{SW}\downarrow\uparrow$ forcing, DH simplified (1) to

$$C\frac{\partial \hat{T}}{\partial t} = A\sin\omega t - b\hat{T}. \qquad (2)$$

Here C is thermal inertia, t is time, b is a positive damping constant, T is SST, $A\sin\omega t$ is the annual harmonic in solar forcing ($\mathrm{SW}\uparrow\downarrow$), and the caret denotes a departure from the yearly mean. The purpose of (2) is to obtain the right SST in response to known forcing. It is not our primary goal to model the heat storage correctly from the interface heat exchange terms only. In (2) all we have to know, in addition to the annual cycle in SST, is the forcing of the annual cycle in SST, that is A; b and C can then be determined empirically. Equation (2) has several advantages. First, one does not need to know the various empirical fluxes combined in $F\downarrow\uparrow$ in (1), except for $\mathrm{SW}\downarrow\uparrow$ which anyway is the easiest of the four to estimate. Second, the solution to (2), i.e. $\hat{T}$, has not been used in evaluating the forc-

ing, so theoretically it is a clean approach. Below we will call (2) Method I and describe how it can be used. For Methods II and III we will utilize the more demanding (and uncertain) knowledge of $F\downarrow\uparrow$ as the forcing in (2).

Method I

Van den Dool and Horel proposed to use (2) to determine the active layer depth. Equation (2) expresses how SST is a response to solar forcing modified by damping, i.e. a linear damped oscillation.

The temperature response to an annual harmonic in the forcing ($A \sin\omega t$) is given by

$$\hat{T} = B \sin(\omega t - \Delta) + C_1 \exp(-bt/C) \quad (3)$$

where

$$\tan\Delta = C\omega/b; \quad 0 \leqslant \Delta < 90° \quad (3a)$$

and

$$B = A/[b^2 + (\omega C)^2]^{1/2} = A \cos(\Delta)/b. \quad (3b)$$

The second term on the right-hand side of (3) obviously vanishes for $t \to \infty$ and need no longer be considered.

Starting from observed values of B, A and Δ (all for the annual harmonic), we will calculate C and b from (3a)–(3b). The procedure is entirely local and the resulting C and b vary in space to the extent that B, Δ and A are a function of space. From C, the active layer depth h can be found from

$$C = \rho c_p h \approx 4.2 \times 10^6 h \quad [\text{J m}^{-2}\,\text{K}^{-1}] \quad (4)$$

where ρ is water density and c_p is specific heat.

In Method I the forcing is assumed to be solar radiation only, taken from an expression given by Seckel and Beaudry (1973). The astronomical solar radiation being denoted by S_a, we assume that only

$$\text{SW}\uparrow\downarrow = S_a(1 - \alpha)\tau \quad (5)$$

is absorbed by the ocean; here τ and α are atmospheric transmission and global albedo, respectively. Under Method I the term $(1 - \alpha)\tau$ is taken to be 0.525, uniform in space and time, a most drastic simplification of the problem. The S_a has been calculated every day, but in order to be consistent with the other data, 12 calendar monthly means were calculated. The annual harmonic was then adapted to the 12 monthly means; this was done at the center of each 5° × 5° box where co-located SST data are available.

It should be noted that using the annual cycle in $\text{SW}\uparrow\downarrow$ excludes the possibility of useful results in areas where the amplitude (A) is too small (near the equator). We arbitrarily set the lowest acceptable A at 10 W m^{-2}. Note also that (2)–(4) do not yield useful results if Δ is either >90° or <0°.

As a further commentary on Method I, we must also point out that Eq. (2) has been used for essentially the same purposes by Frankignoul and Hasselmann (1977). While we use (2) to extract C and b from the deterministic annual signal at one frequency only, they use (2) in a stochastic manner. By discarding phase information and applying (3b) to the whole spectrum of SST anomalies, the ratio $\lambda = b/C$ can be determined. Frankignoul and Reynolds (1983) determined λ for the northern Pacific Ocean (their Fig. 7) and the agreement with DH's b/C is striking, both in pattern and in magnitude. Apparently the linear feedback coefficient acting on stochastic anomalies at time-scales ranging from 2 months to 28 years is rather similar to λ acting on the deterministic annual cycle.

Method II

This is identical to Method I, except that $\text{SW}\downarrow\uparrow$ is here given by Bunker's empirical procedure that depends on S_a and location dependent cloud cover (Lamb and Bunker 1982). This dataset will be referred to as "observed" solar radiation.

Clouds may considerably change the annual cycle in $\text{SW}\downarrow\uparrow$, so Method II should be an improvement over Method I in several respects. In DH it was speculated that the poor results in the subtropical East Pacific (Δ > 90 days) were due to the fact that stratus and fog in May and June postpone the moment of maximum forcing until July. This speculation will be tested here with data for the Atlantic, where fog and stratus off the west coast of Africa are equally common.

Method III

An obvious problem with our use of (2) thus far is the arbitrary assumption that solar radiation forces the annual SST cycle and "everything else" damps it back to equilibrium. For the sake of argument, we shall from now on define forcing as any process that, when prescribed in isolation, results in high SST in summer and low SST in winter. On the other hand, a damping process reduces the observed annual cycle in SST. Clear examples of forcing and damping are solar radiation and upward infrared radiation, respectively. The processes we have hitherto lumped into the damping parameter b in (2) represent (i) downward atmospheric infrared flux, (ii) upward infrared flux from the ocean surface, (iii) net upward fluxes of latent and sensible heat (LE, SH), and (iv) the combined effect of horizontal and vertical (i.e., entrainment, turbulent mixing) oceanic transport of heat (OTR). Judging from Hastenrath and Lamb (1978), however, very few of these processes actually damp the annual cycle in SST. We therefore now drastically combine all the fluxes at the ocean–atmosphere interface into one "forcing." Equation (2) can then be rewritten as

$$C^* \frac{\partial \hat{T}}{\partial t} = A^* \sin\omega t - b^* \hat{T} \quad (6)$$

where A^* is the amplitude of the annual harmonic in

the net energy flux at the surface ($F\downarrow\uparrow$) and the b^* parameter therefore represents only lateral and vertical ocean heat transports. Whether (6) is a more meaningful separation into forcing ($\hat{F}\downarrow\uparrow$) and damping ($b^*\hat{T}$) remains to be seen. According to Bryan and Schroeder (1960), the ocean heat transport actually forces the annual cycle in SST between 20°N and 55°N in the Atlantic, so representing OTR as a damping might not be completely appropriate.

3. Data

This study uses four sets of data (SST, SW$\uparrow\downarrow$, $F\downarrow\uparrow$, mixed layer depth) derived from Lamb and Bunker (1982) and Lamb (1984). All sets contain calendar monthly means for 5° latitude–longitude areas for the 70°N–20°S domain.

The SST, SW$\uparrow\downarrow$ and $F\downarrow\uparrow$ averages are based on ~7.8 million sets of surface marine meteorological observations for the period 1948–72. This dataset was originally developed by Andrew F. Bunker (Woods Hole Oceanographic Institution), who also performed the basic sea–air heat flux calculations utilized here. Detailed information on those subjects appears in Bunker (1976, 1980, 1988), Bunker and Goldsmith (1979), and Bunker and Worthington (1976). See Lamb and Bunker (1982) for information on how this basic material was distilled into the above datasets for SST, SW$\uparrow\downarrow$ and $F\downarrow\uparrow$.

The mixed layer depth (h_m) averages used here were derived from an analysis of ~234 000 individual subsurface temperature soundings for the period 1967–76. In this analysis, the mixed layer base was taken to be the level at which the temperature was 1°C less than at the surface. See Lamb and Bunker (1982) and Lamb (1984) for details concerning the development of the subsurface temperature dataset and its use to identify the mixed layer depth. For the mixed layer depth in the tropical Atlantic Hastenrath and Merle (1987) used an even more extensive data bank than Lamb (1984). Nevertheless the annual mean h_m used here for verification, is very close to Hastenrath and Merle's.

4. Results

a. Method I

Figure 1 shows the amplitude (B) of the annual harmonic in (observed climatological) SST over the Atlantic Ocean and adjacent gulfs and seas. Close to the equator B is very small, while B is very large just off the North American continent ($B > 7$ K). This distribution of B will be considered "the response" for Methods I, II and III. In midlatitudes the annual harmonic explains over 90% of the variance of the climatological annual variation in SST (Levitus 1987a). The pattern of B is very similar to that in the Pacific (See Fig. 1 in DH). The biggest problem for Method I will occur in the eastern tropical Atlantic where B is large in some areas off the African coast (up to 3 K) even though the solar forcing at those latitudes has only a very small annual component. The greatest challenge is to explain the zonal asymmetry in B in midlatitudes. Under Method I the forcing is zonally

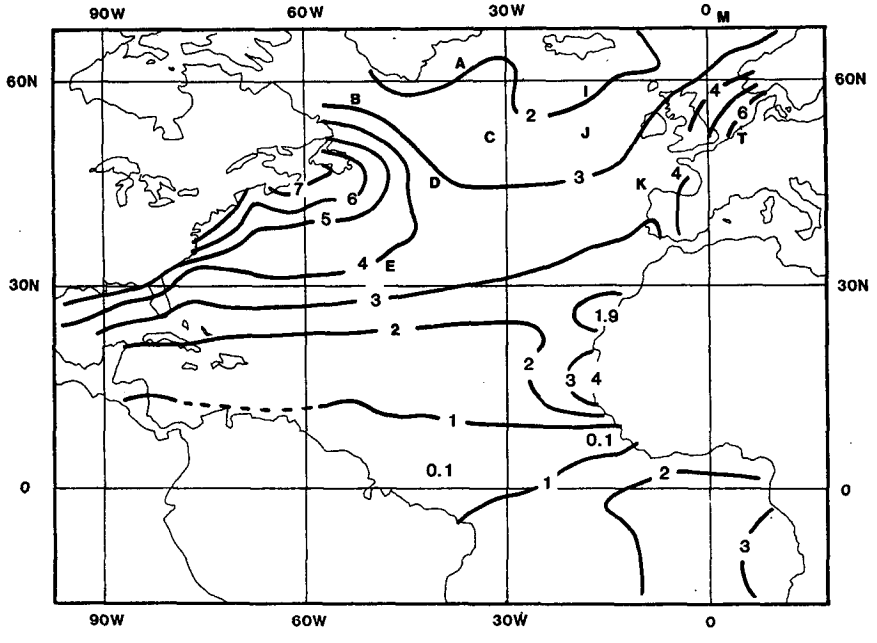

FIG. 1. The amplitude (B) of the annual harmonic in SST. Unit: K. Because the basic data consists of 5° × 5° latitude–longitude boxes some isolines run over land in this and all subsequent figures. At the positions denoted by A · · · T, ocean weather ship data are available.

symmetric and therefore the zonal asymmetry in B must result from spatial variations in b or C, or b and C.

Using Method I the amplitude and phase of the annual cycle in SW$\uparrow\downarrow$ are a function of latitude only. The amplitude varies from less than 2 W m^{-2} just north of the equator to more than 120 W m^{-2} at 60°N. The date at which SW$\uparrow\downarrow$ is highest in the Northern Hemisphere is spatially almost constant (June 21 ± 2 days). Neither of these astronomical input patterns need to be shown.

Figure 2 shows the delay of SST behind the astronomical solar radiation. The lag (Δ) varies from 50 days (Gulf of Mexico, North Sea), through 70 (over most of the open Atlantic) to more than 100 days in the eastern subtropical Atlantic of both hemispheres. The Δ is not displayed where $A \leq 10$ W m^{-2}, that is in a zonal strip centered slightly north of the equator. Figure 2 has much in common with the corresponding map for the Pacific (Fig. 2 in DH), even to the extent that it has problems ($\Delta > 90$ days) in the eastern subtropical oceans. It must be pointed out, however, that Δ is much smaller in the seas south of Iceland than at high latitudes in the Pacific.

The amplitude and phase of the annual cycle in SST (Figs. 1 and 2) are based on all observations made within 5° × 5° boxes. There are only a few locations (ocean weather ships, light vessels) where A and Δ can be calculated from local time series. The comparison is given in Table 1. Generally speaking the values in Table 1 indicate that the amplitude and phase in Fig. 1 and 2 may be off by only a few tenths °C and a few days respectively. This would certainly be acceptable if the errors were random. Unfortunately it seems that in Fig. 1 we generally underestimate slightly the true amplitude, while in Fig. 2 we slightly overestimate the delay Δ. A comparison with Levitus (1987a) also gives the impression of small but systematic differences. Apparently the horizontal averaging within 5° × 5° boxes makes the ocean response seem slower than actually occurs. (A small bias of the same nature is also introduced by using monthly means.)

From Figs. 1 and 2 and the astronomical input data for SW$\uparrow\downarrow$, b and h have been calculated using (3a), (3b) and (4). Areas where either $A \leq 10$ W m^{-2} or $\Delta > 90$ days are not analyzed in Figs. 3 and 4 (i.e., the tropical strip and eastern subtropics). Figure 3 displays the result for b, the damping coefficient. While $5 < b < 15$ over most of the subtropical Atlantic, the inferred damping is very large in high latitudes, $b > 30$ W m^{-2} K^{-1}. The very high value for b coincides with an area visited frequently by strong cyclones and strong surface winds. Figure 3 has much in common with the distribution of b over the Pacific (see Fig. 3 in DH), except for the very large magnitudes near Iceland. This difference is perhaps associated with the vigorous deep-water formation in the Atlantic at these high latitudes, a process absent in the Pacific.

The calculated active layer depth as inferred from (3a), (3b) and (4) is shown in Fig. 4. The depth, h, varies from less than 20 m in the coastal waters (a reassuring feature) to more than 60 m southwest of Iceland. The few gridpoints at low latitudes where both $A \geq 10$ W m^{-2} and $\Delta < 90$ days indicate that the active

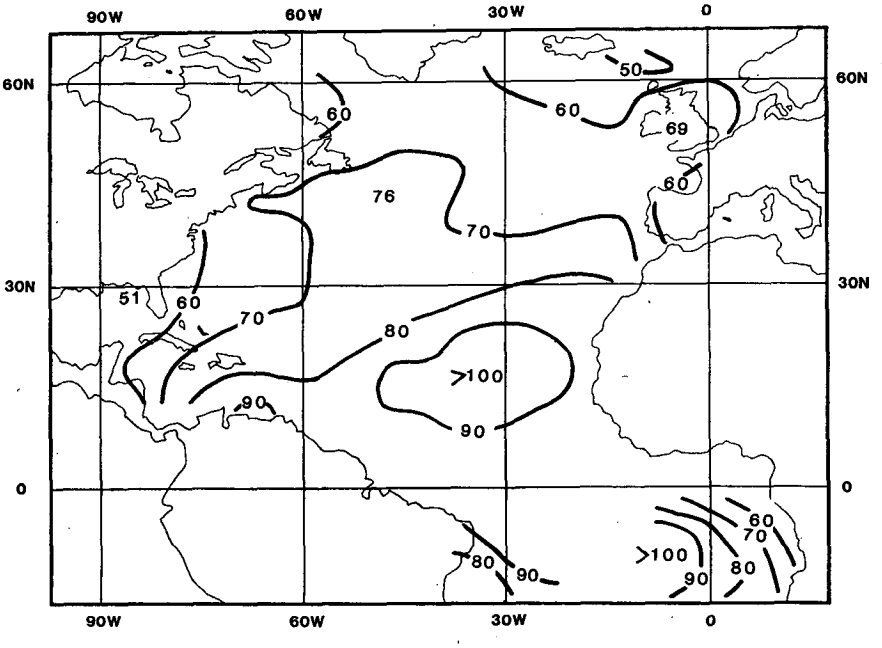

FIG. 2. The delay (Δ) of the annual harmonic in SST behind the astronomical solar radiation. Unit: days. No delays are shown where the amplitude of the annual harmonic in solar radiation is less than 10 W m^{-2} K^{-1}.

TABLE 1. The amplitude and phase (relative to June 21) of the annual harmonic in climatological sea surface temperature at the site of nine ocean weather ships (A–M) and a light-vessel in the North Sea (T). The in-situ data are for 1951–60 (ships) and 1890–75 for the light vessel. The right most two columns give the difference between in situ values and those analyzed in Figs. 1 and 2.

Ship	Lat Long	Amplitude A (K)	Phase Δ (days)	In situ − analysis A (K)	In situ − analysis Δ (days)
A	62°N 33°W	2.7	53	+0.8	−7
B	57°N 51°W	3.1	62	+0.2	0
C	53°N 35°W	3.0	60	+0.4	−8
D	44°N 41°W	3.1	70	0.0	−1
E	35°N 48°W	4.2	73	+0.5	−2
I	59°N 19°W	2.1	60	+0.3	+5
J	52°N 20°W	2.3	58	0.0	−3
K	45°N 16°W	3.3	63	0.0	0
M	66°N 02°E	2.6	59	+0.2	+4
Light Vessel *Texel*	53°N 04°E	6.2	58	0.0	0

layer may be as shallow as 5 meters just off the African coast. Figure 4 is rather similar to Fig. 4 in DH, for the Pacific, where h ranges from 15 to over 60 meters. Figure 4 should also be compared to the observed annual mean mixed layer in the Atlantic as computed from the six bimonthly patterns of Lamb (1984) and presented here in Fig. 5. As was the case for the Pacific, h is less than half the depth of the observed mixed layer. But the patterns in Figs. 4 and 5 are reasonably similar, indicating that, by and large, Method I has some validity. It is truly surprising that an equation as simple as (2), driven by the crudest possible assumptions about solar forcing, yields an essentially correct description of the topography of h_m. The pattern correlation between Fig. 4 and 5 is 0.65.

b. *Method II*

We will now investigate whether replacing "astronomical" by "observed" SW↑↓ improves any of the problems and discrepancies noted above. First, we will discuss the changes in A and Δ that result from taking clouds empirically into account in the SW↓↑ estimates. Figure 6 displays the percent change in the amplitude of the annual cycle in SW↑↓ relative to its astronomical value. Except for the area of the subtropical highs the astronomical amplitude was apparently an overestimate, by as much as 50% southeast of Greenland. This result is reasonable since the subtropics have less clouds and the midlatitudes have more clouds (year round) than was assumed in taking $\tau(1 - \alpha) = 0.525$ everywhere. Note that clouds reduce the north–south gradient in A, while maintaining near perfect zonal symmetry in forcing in the central North Atlantic. The change in Δ as a result of clouds is given in Fig. 7. As can be seen, the moment of highest solar radiation can be shifted by as many as 15 days forward (negative values) and backward (positive values) relative to June 21, as a result of clouds. The largest (expected) shift occurs in the eastern subtropical ocean where clouds displace the moment of highest (and lowest!) insolation forward by more than 20 days.

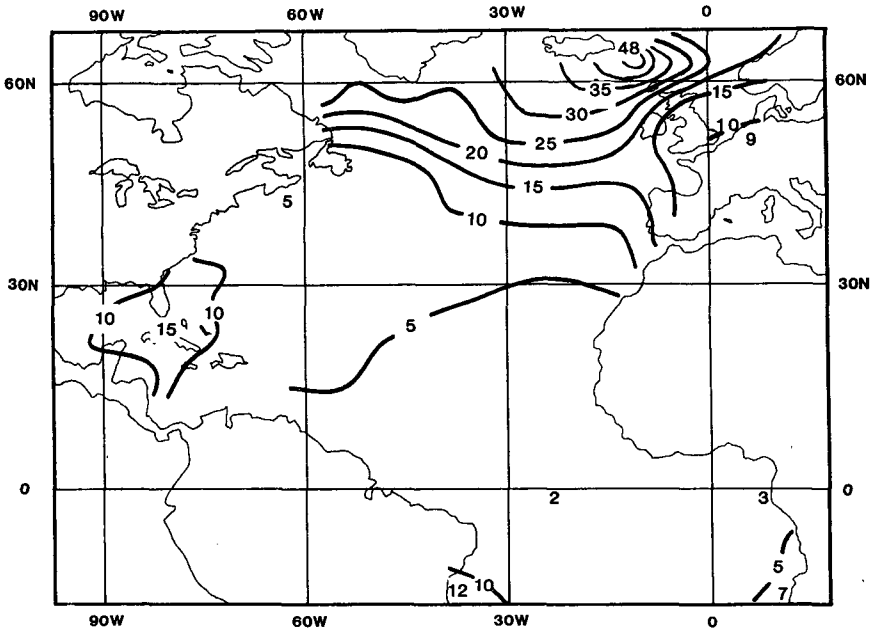

FIG. 3. The damping coefficient b, in W m^{-2} K^{-1}, as calculated from Eqs. (3a), (3b) and (4) and Figs. 1 and 2 (Method I).

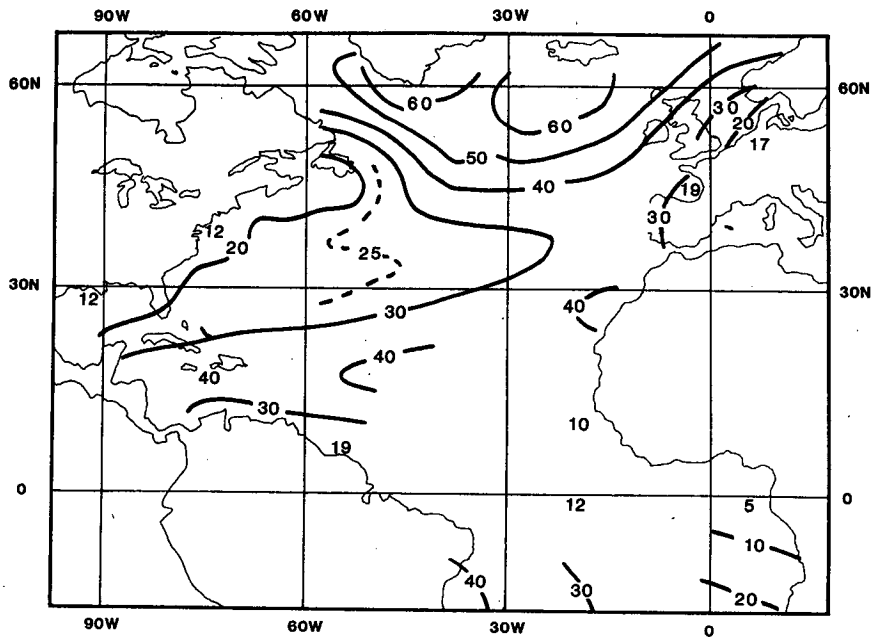

FIG. 4. The active layer depth h, in meters, as calculated from Eqs. (3a), (3b) and (4), and Figs. 1 and 2 (Method I).

Method II should be an improvement over Method I, because the cloud impact on A seems reasonable and because the area where $\Delta > 90$ days has shrunk considerably. Of course these improvements may be only qualitative in nature. Moreover, because $A \leq 10$ W m^{-2} over a much larger area now, a meaningful analysis is possible in only a few squares south of 25°N.

Figures 8 and 9 show b and h according to Method II. Although the large-scale pattern has not changed very much, we note the following differences: (i) b is no longer excessive in the high latitude areas, and (ii) the active layer is even shallower now than previously. Comparing Figs. 4, 5 and 9 it cannot be concluded that as a result of taking clouds into account h matches the

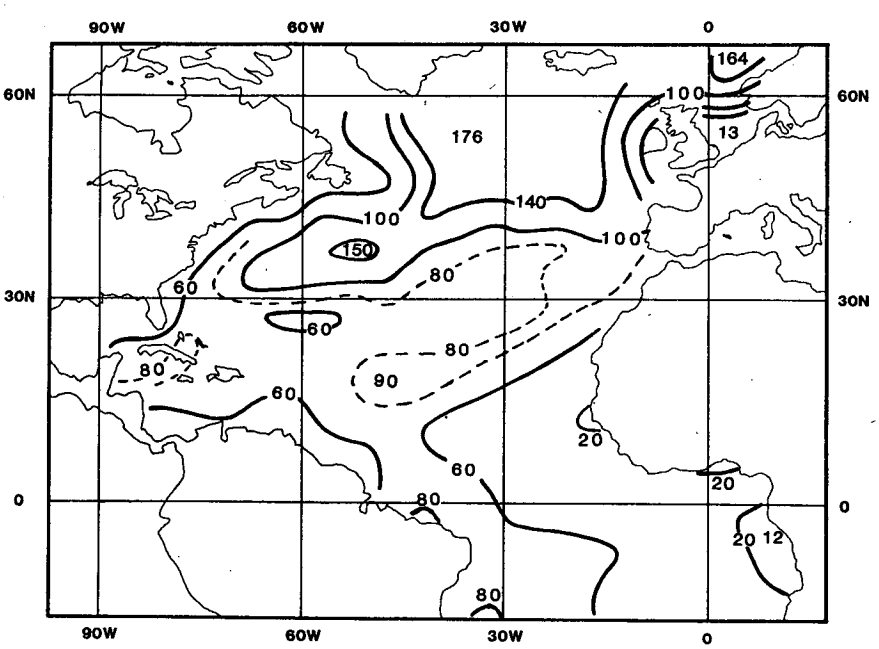

FIG. 5. The annual mean observed mixed layer depth in the Atlantic according to Lamb (1984). Unit: meters.

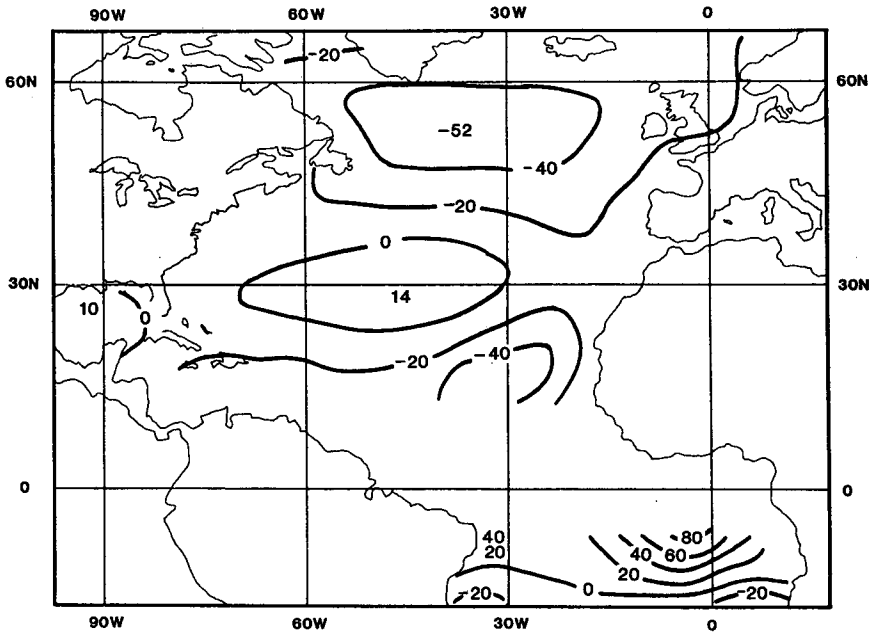

FIG. 6. The percent change in the amplitude (A) of the annual harmonic in absorbed solar radiation due to clouds.

observed mixed layer depth pattern any better—certainly not in magnitude!—while the topographic match has also deteriorated. The pattern correlation between Figs. 9 and 5 is only 0.40, down from 0.65 when astronomical SW↑↓ was used.

c. *Method III*

We will now discuss Method III, the inversion of (6), in some detail. The forcing here consists of $F\downarrow\uparrow$, which is far more complete than just solar radiation.

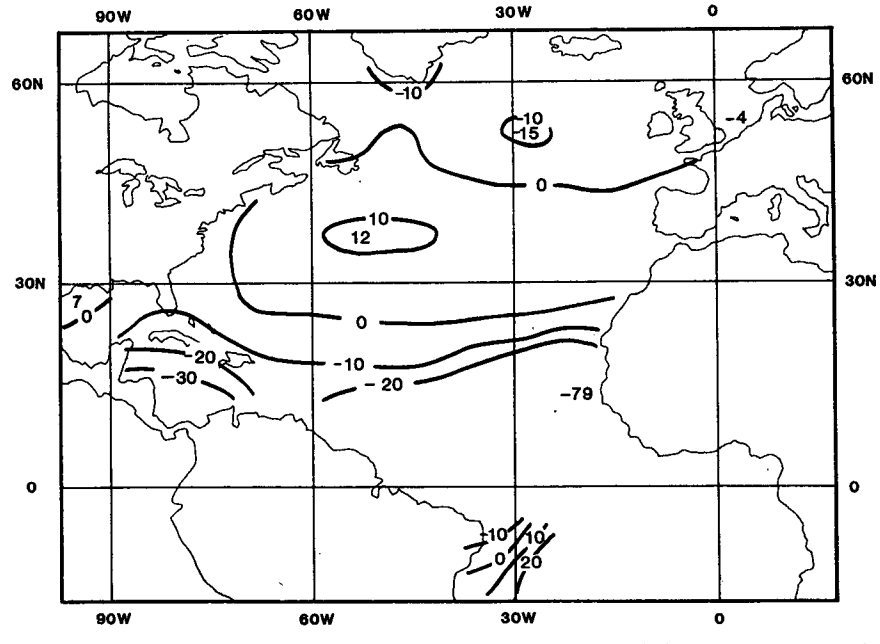

FIG. 7. The change in phase of the annual cycle in absorbed solar radiation due to clouds. Unit days. Example, −15 means that the highest value is reached on 6 July rather than 21 June.

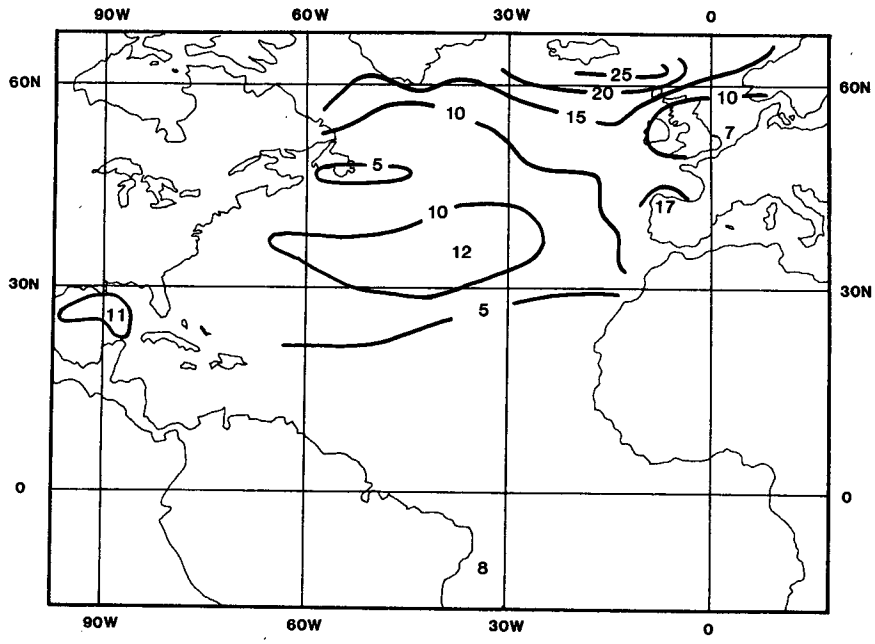

FIG. 8. As in Fig. 3 but for "observed" solar radiation (Method II).

The danger, however, is that we have to rely on the accuracy of empirical formulae. Also we have lost the purity of (2), because the solution has been used to evaluate the forcing.

Figure 10 shows A^*, the amplitude of the annual harmonic in $F\downarrow\uparrow$. Some of the zonal symmetry of the astronomical solar forcing is still preserved at low latitudes, with A^* being somewhat larger than A nearly everywhere. In the trade wind regimes $A^* > A$ because the evaporation cools the ocean more in winter than in summer (Hastenrath and Lamb 1978). The largest modification of A by interface heat fluxes other than SW$\downarrow\uparrow$ occurs off the North American continent where the outbreak of continental air masses amplifies A from

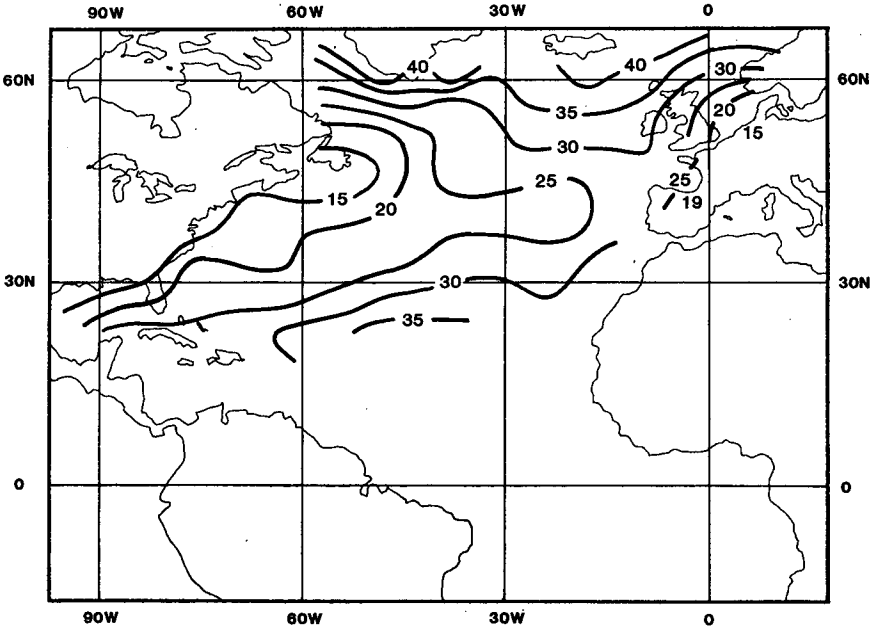

FIG. 9. As in Fig. 4 but for "observed" solar radiation (Method II).

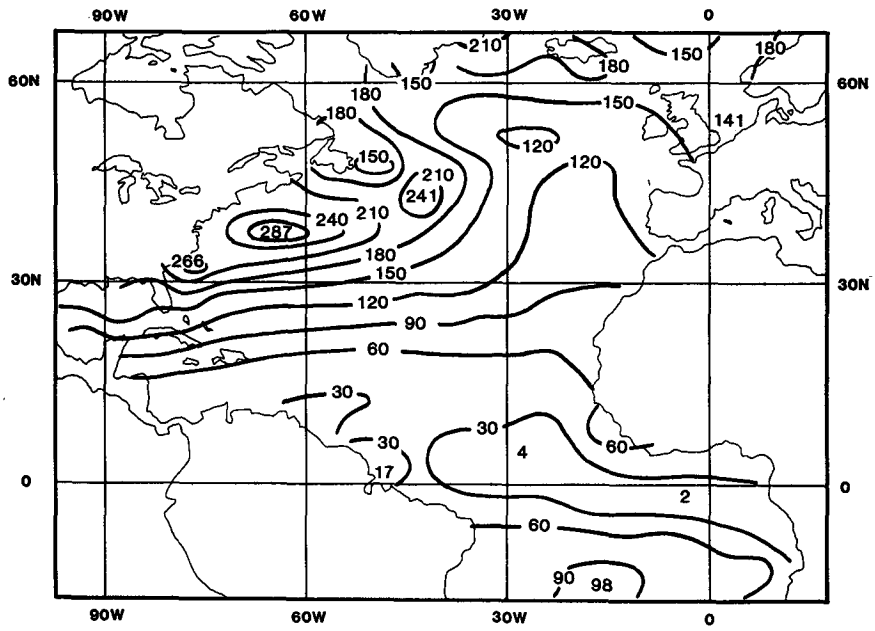

FIG. 10. The amplitude (A^*) of the annual harmonic in the net surface ocean heat gain ($F\downarrow\uparrow$). Contour interval 30 W m^{-2}. Input data for Method III.

about 100 to more than 200 W m^{-2}. Forcing (Fig. 10) and response (Fig. 1) are very similar now (perhaps more so than they should be). This is because SST enters LW$\downarrow\uparrow$, LE and SH thereby forcing A^* to be similar to B. Notice, however, that the maximum value of A^* in Fig. 10 does not exactly coincide with maximum response B in Fig. 1, and also that A^* has more small scale structures and huge gradients off the North American coast.

The delay of SST behind $F\downarrow\uparrow(\Delta^*)$ is shown in Fig. 11. The delay is generally 10 days less than in Fig. 2, indicating that $F\downarrow\uparrow$ reaches its maximum around July

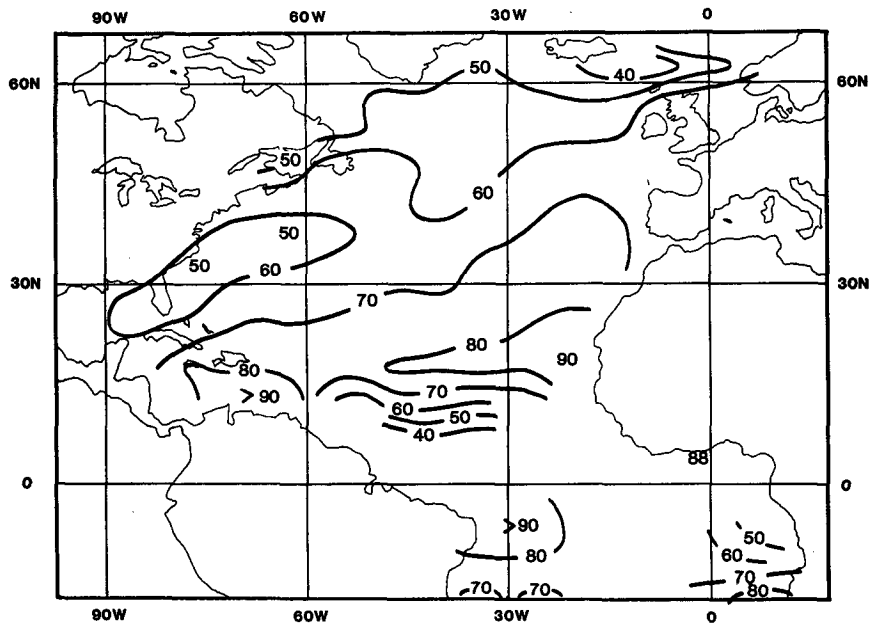

FIG. 11. As in Fig. 2 but now behind the net ocean surface heat gain. Unit: days. Input data for Method III.

1. The problem area where Δ is larger than 90 days in Fig. 2 is therefore greatly reduced. From the fact that Δ^* is substantially smaller than 90° it follows that the implied damping term is large. Negligible damping in (6) would imply $\hat{T}$ to be 90° out of phase with the forcing. Both Figs. 10 and 11 are slightly noisier than Figs. 1 and 2. This is due to the details in the LE flux pattern in particular.

Using Figs. 1, 10 and 11 as input, we can now invert (6) to obtain b^* and h^*. Results are displayed in Figs. 12 and 13. Those concerning b^* (Fig. 12) suggest that the damping is much larger than depicted in Fig. 3. Similarly, in Fig. 13, h^* is 1.5 to 2 times deeper in the West Atlantic than it was in Fig. 4, where only astronomical solar forcing was used. The pattern morphology of h^* has also changed mildly relative to h and, as in the h_m observations (Fig. 5) we now see in Fig. 13 the deep active layer extending southwestward from the vicinity of Iceland up the Gulf Stream and into the Caribbean Sea.

d. Intercomparison

In Table 2 we compare the depth of the observed annual mean mixed layer (Fig. 5) to the depth of active layer calculated by the Methods I, II and III. The comparison is made by calculating the pattern correlation coefficient (PCC) with each 5° × 5° square being weighted by the cosine of the latitude. The PCC measures pattern similarity and as can be seen, Method I yields the h field that is most similar to the h_m field, both over the entire domain (PCC = 0.65) and over midlatitudes (PCC = 0.68). Method III is nearly as good, while modifying only the solar radiation by clouds (Method II) is a deterioration. Table 2 also gives the spatial mean h (for each method and domain), the spatial mean h_m for each domain, and their spatial standard deviations. All methods indicate that h is at most only about half as deep as h_m. One reason that the highest PCC in Table 2 is not higher than 0.68 is that the observed h_m contains more small scale information ($sd_h \approx 10$–15, $sd_{h_m} \approx 45$). So, even though Methods I, II and III are local in their approach, the resulting active layer is of a very large spatial scale. Therefore, correlations of 0.6 to 0.7 are quite satisfactory. Applying a 9-point spatial filter twice to the h_m field improves the correlations (although not the statistical significance) for all methods and all areas. For example the aforementioned PCC = 0.68 (Table 2, Method I, midlatitudes) increases to 0.72.

e. Zonal mean results

As a summary of the results so far, zonal averages are presented in Table 3. We have tabulated as a function of latitude the following quantities—the amplitude of the annual harmonic in zonal mean SST; the amplitude of the annual harmonic in the zonal mean forcing for Methods I, II, III; the delay of the temperature behind the forcing (I, II, III); and the resulting damping coefficient and active layer for Methods I, II and III. Finally, the observed zonal and annual mean mixed layer depth is given.

It is clear that going from astronomical to observed solar radiation (SW↓↑) reduces A, makes the calculated active layer shallower, and does not resolve the issue

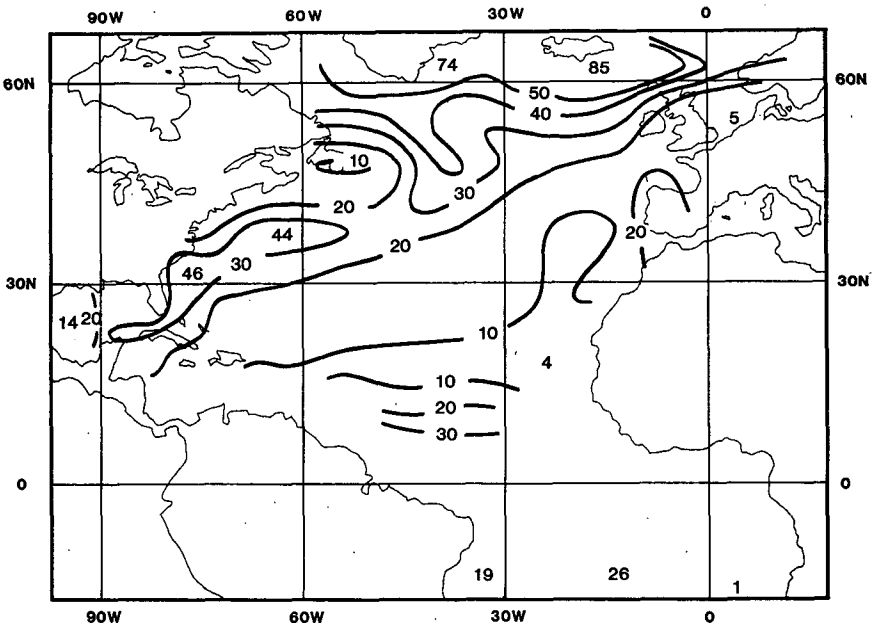

FIG. 12. The damping coefficient b^* calculated according to Method III. Unit: W m^{-2} K^{-1}.

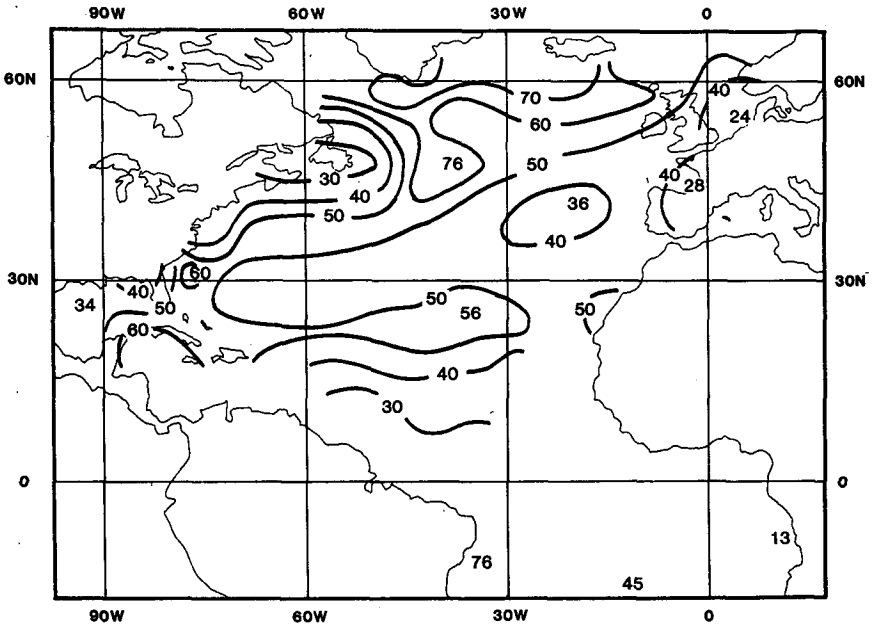

FIG. 13. The active layer depth h^* (in meters) according to Method III.

as to why the active layer is shallower than the mixed layer. Using the net surface oceanic heat gain ($F\downarrow\uparrow$), as calculated from net short- and longwave radiation and the sensible and latent heat fluxes, a substantially deeper active layer is found. The somewhat closer agreement between the magnitudes of h and h_m under Method III is the result of an increased forcing amplitude A^*. This is almost entirely due to the annual cycle in evaporation which acts so as to force the annual cycle in SST. This "observational fact" depends on the validity of the expression

$$\mathrm{LE} = L\rho_a C_D |\mathbf{V}| (q_s - q_a) \qquad (7)$$

TABLE 2. Pattern correlation coefficient (PCC) between observed annual mean mixed layer depth (h_m, Fig. 5) and calculated active layer (h) according to the three methods. In the upper part all 5° × 5° squares within 20°S ≤ ϕ ≤ 70°N are used for the calculation, while in the lower part only those within 20°N ≤ ϕ ≤ 60°N are used. Weighted spatial means of h and h_m, spatial standard deviations of h and h_m, and N, the number of 5° × 5° boxes that entered the calculation, are tabulated as well. N is the number of boxes where $A \geq 10$ W m^{-2} and $0 < \Delta \leq 85$ days. Therefore N (and h_m) is slightly method dependent.

		PCC	N	$\bar{h}$	$\bar{h}_m$	sd_h	sd_{h_m}
Whole domain	I	0.65	205	30 m	75 m	14 m	46 m
	II	0.40	160	26	85	9	49
	III	0.56	214	45	76	16	44
20°N ≤ ϕ ≤ 60°N	I	0.68	124	31	85	12	43
	II	0.41	119	25	86	7	43
	III	0.60	125	47	85	11	43

in climatological applications. In (7), $(q_s - q_a)$ is the near-surface gradient of specific humidity, $\mathbf{V}$ is the surface wind vector, C_D is a dimensionless exchange coefficient and ρ_a is air density. Hastenrath and Lamb (1978) explain that the large annual cycle in LE over large areas is primarily produced by strong (weak) winds in winter (summer).

However, even under Method III, h is substantially smaller than h_m. It is unlikely that the horizontal and vertical oceanic heat transports provide additional forcing of sufficient magnitude (Bryan and Schroeder 1960; Gill and Niiler 1972; Hall and Bryden 1982). It follows that the depth of the active layer is only about half that of the mixed layer.

f. Using the second harmonic

In some areas the amplitude of forcing at the annual frequency is too small to expect any results from Eqs. (2) and (6). In particular this is the case close to the equator where the first harmonic nearly vanishes. As an alternative, we report here the results from using the second harmonic. As shown in Table 4, the forcing (under Method I) reaches 12 W m^{-2} at 2.5°N. The response in SST at these low latitudes is only 0.4 K so it is not easy to extract accurate information about h and b employing the second harmonic. Note that Table 4 is confined to zonal average results. At many latitudes either $\Delta > 45$ days or $A < 10$ W m^{-2}, so very few values of b and h can be determined. At 17.5°N we find $b = 18$ W m^{-2} K^{-1} and $h = 21$ m, which is in very poor agreement with the nearest result obtained

TABLE 3. Results of inverting (2) or (6) by using the annual cycle (first harmonic) in zonal mean SST and zonal mean forcing. The forcing has been calculated according to Methods I, II and III and hence there are 3 forcing amplitudes A, 3 delays Δ, 3 damping coefficients b, and 3 active layers h. The last column is the zonal mean annual mean observed mixed layer derived from Lamb (1984). The latitude indicated is the center of a 5° latitude strip covering the Atlantic Basin. Results of the calculations are not shown if either $A < 10$ W m^{-2}, $\Delta < 0$ or ≥ 85 days.

		A (W m^{-2})			Δ (days)			b (W m^{-2} K^{-1})			h (m)			
Latitude	B (K)	I	II	III	I	II	III	I	II	III	I	II	III	h_m (m)
67.5N	1.4	124	98	178	71	74	56	31	21	72	98	79	123	128
62.5	2.2	124	91	177	53	57	40	34	23	62	54	41	61	166
57.5	2.8	121	73	155	61	65	56	21	11	32	45	28	54	128
52.5	3.5	116	73	142	62	66	59	16	9	22	35	23	42	94
47.5	4.3	110	78	157	66	64	60	11	8	18	28	19	38	105
42.5	4.5	102	82	171	68	64	63	9	8	18	25	19	40	102
37.5	4.2	92	85	181	67	61	59	9	10	23	24	21	44	90
32.5	3.8	80	79	157	66	62	64	9	10	19	23	22	44	82
27.5	3.0	68	68	127	68	66	66	9	9	18	25	25	46	64
22.5	2.0	55	50	93	73	79	72	8	5	15	31	29	52	70
17.5	1.6	42	30	53	—	—	—	—	—	—	—	—	—	70
12.5	1.4	28	20	28	—	—	—	—	—	—	—	—	—	49
7.5	0.1	14	19	10	—	—	—	—	—	—	—	—	—	42
2.5	0.9	2	9	17	—	—	—	—	—	—	—	—	—	45
−2.5	1.8	15	6	13	—	—	—	—	—	—	—	—	—	45
−7.5	1.9	29	34	55	—	—	68	—	—	11	—	—	31	53
−12.5	2.0	43	46	79	—	—	66	—	—	17	—	—	43	53
−17.5S	2.2	57	46	76	80	51	72	5	13	11	30	19	39	59

for the first harmonic at 22.5°N. A second harmonic in T could be the (linear) result of a second harmonic in the forcing, or the nonlinear result of C being season dependent. The latter nonlinearity can only be neglected in some areas where C is independent of season (low latitudes), but unfortunately no credible values of b and h can be obtained there. So, there is not much utility for our purpose in the second harmonic.

TABLE 4. As in Table 3 but now for the second harmonic and Method I only. Results of the calculations are suppressed (—) if either $A < 10$ W m^{-2} or $\Delta < 0$ or $\Delta \geq 45$ days.

Latitude (deg)	B (K)	A (W m^{-2})	Δ (days)	b (W m^{-2} K^{-1})	h (m)
67.5	0.8	27	19	27	12
62.5	0.7	18	43	2	16
57.5	0.5	12	42	3	13
52.5	0.5	7	40	—	—
47.5	0.8	3	25	—	—
42.5	0.7	2	—	—	—
37.5	0.5	4	—	—	—
32.5	0.3	6	—	—	—
27.5	0.1	8	—	—	—
22.5	0.2	9	26	—	—
17.5	0.3	10	32	18	21
12.5	0.4	11	49	—	—
7.5	0.4	11	—	—	—
2.5	0.4	12	46	—	—
−2.5	0.5	11	31	11	12
−7.5	0.3	11	30	20	20
−12.5	0.2	10	17	—	—
−17.5	0.1	9	13	—	—

g. *Deterministic versus stochastic forcing*

Figure 14 shows $\lambda^{-1} = C/b$ in units of months as calculated from Method I. Although derived from the phase locked deterministic annual cycle we present λ^{-1}, the feedback constant (Frankignoul and Reynolds 1983) as if it would apply also to the decay of stochastically forced SST anomalies. The interpretation of Fig. 14 therefore is that the e-folding time of SST anomalies is 2–3 months in the Gulf of Mexico, the North Sea and the Gulf of Biscay, up to 6 months well off the North American coast at 45°N, and even longer in the eastern Subtropical North Atlantic. For the Pacific, λ derived from the phase-locked annual cycle (DH) and the stochastic method (Frankignoul and Reynolds 1983) compared quite well. To our knowledge the e-folding time of SST anomalies in the Atlantic (from direct calculation) has not been published so we can not, as yet, verify the applicability of Fig. 14 to SST anomalies.

We use Method I to show λ^{-1} because Method I is the simplest and at least as good in calculating C as Method III. Note, moreover that λ does not depend on the amplitude (A) of the forcing, but only on the phase (Δ) which is not too different for Methods I and III.

5. Conclusions and discussion

The purpose of this paper was twofold. First it extended the approach suggested by Van den Dool and Horel (1984) to the Atlantic Ocean. They proposed to

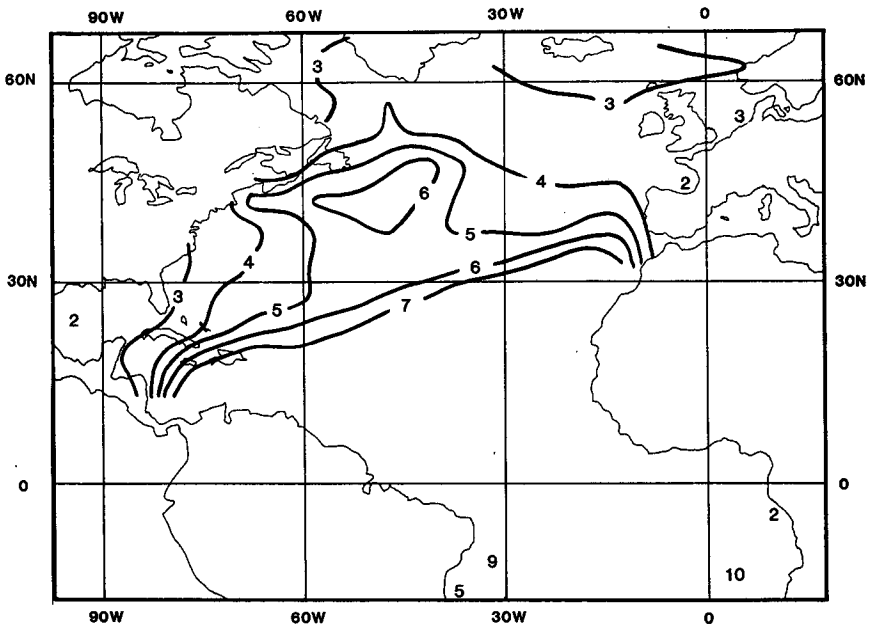

FIG. 14. The damping time scale C/b in units of months for Method I.

exploit the annual cycle in SST as a well-documented example of climate change. Assuming that SST is governed by a simple energy balance equation, the two constants (thermal inertia C and damping parameter b) in that equation can easily be determined. Van den Dool and Horel applied this method to the North Pacific. Second, since a thoroughly analyzed climatology of air–sea fluxes was available for the Atlantic Ocean (Lamb and Bunker 1982), some of the assumptions underlying DH's simple energy balance were investigated. In particular, their assumption that processes either force (solar radiation) or damp ("everything else") the annual cycle in SST, could be relaxed, as all interface heat fluxes were available (not so for the Pacific).

It was found, nevertheless, that the results for the Atlantic are very similar to those obtained for the Pacific (in DH). The assumptions made by DH were apparently not too damaging to their final conclusions. In some detail the present conclusions are as follows.

1) Assuming a simple energy balance, Eq. (2), and assuming that the "astronomical" solar radiation forces and "everything else" damps the annual cycle in SST, an active layer depth (h) was calculated for the Atlantic which patternwise was found to be rather similar (pattern correlation ~ 0.7) to the annual mean mixed layer depth (h_m).

2) However, in magnitude h is found to be substantially less than h_m, which is in agreement with DH's results for the Pacific.

3) Changing the solar forcing so as to empirically include, the modifying effects of clouds did not lead to better agreement between h and h_m (neither in pattern, nor in magnitude). This may cast some doubt on the (quantitative) accuracy of the empirical formula used by Lamb and Bunker (1982).

4) Enriching the forcing to empirically include all interface fluxes yielded a slightly better agreement for the magnitude of h (vs h_m), but the pattern match did not improve. Again, some doubt exists about the accuracy of empirical estimates of heat fluxes.

5) Regardless of the forcing used, h seems to be shallower than h_m everywhere, on the order of 40–80% of h_m.

6) The damping constant b is very large. Depending on assumptions, b ranges from 5 to over 50 W m^{-2} K^{-1}.

Several global atmospheric models (e.g., NCAR-CCM, GFDL-GCM, NASA-GISS) have been run for very long integrations to assess likely climatic effects of doubling the CO_2 content of the atmosphere (Manabe and Stouffer 1980; Meehl and Washington 1985). The above conclusions indicate that the ocean slab coupled to these atmospheric models should be chosen to be rather shallow, in order to produce realistic SST in response to realistic air–sea heat fluxes. It is easy to understand why $h < h_m$. From our study, as well as Bryan and Schroeder (1960) and Lamb and Bunker (1982), it appears that the annual cycle in the net surface heat gain is too small to fully explain the annual cycle of heat stored in the upper ocean. Specifically, in Fig. 10 A^* would have had to be over 300 W m^{-2} to explain observed storage in some areas (Levitus 1987b). Therefore, in the absence of ocean transport,

the slab should be kept rather shallow if realistic SST is desired.

Even if ocean heat transport was entirely negligible we would expect $h \leqslant h_m$. This is because the oceanic mixed layer is not perfectly mixed all the time. Even with strong surface winds the upper ocean is observed not to be stirred all the way down to h_m, at least not in the daytime (Leetmaa and Welch 1972).

Consistent with $h < h_m$ is the implication that the ocean's heat transport apparently contributes to force the annual SST cycle in midlatitudes of the Atlantic. This implication is very much dependent on the accuracy of the empirical estimates of air–sea heat exchange. While the accuracy is uncertain it is noteworthy that other methods yielding ocean transport as a residual (Carissimo et al. 1985) point in the same direction.

The issue of the accuracy of empirical estimates of SW$\downarrow\uparrow$, LW$\uparrow\downarrow$, SH and LE in Eq. (1) is rather puzzling. While the annual means may seem reasonable, the amplitude of the true annual cycle in net ocean heat gain may be small compared to the uncertainties in the amplitudes of the annual cycle of the individual fluxes. If accurately known input data were available, Method II and most certainly Method III should have been an improvement over Method I (astronomical forcing only). There is probably too much spatial detail in A^* (Fig. 10) for Method III to be an improvement (in terms of comparing h to h_m). With regard to "improving" the estimates of solar radiation reaching the surface by allowing for clouds (Method II), we note the almost complete absence of observations needed to calibrate empirical expressions for SW$\downarrow\uparrow$ over the ocean (see Dobson and Smith 1988 for a few observations). On the other hand, the comparison of h to h_m is not necessarily the ultimate test to decide which of the forcings is most accurately known.

Certainly the first author is happy to see that Eq. (2) is reasonably accurate. In Eq. (2) we have an unambiguous distinction between forcing (SW$\downarrow\uparrow$) and response (in SST). So under Method I the forcing is not influenced by the solution, and therefore provides the "cleanest" model for understanding. Under Method III the solution (as observed) is used to calculate the forcing, thereby artificially improving the performance of Method III. One could argue that even the atmospheric clouds are a response to the ultimate forcing of the annual cycle and should not be included into the forcing.

A discussion about the depth of the active layer seems relevant to modeling only as long as we couple atmospheric models to simple ocean slab models. In fact, some experiments have gone far beyond that. For example, Bryan and Spelman (1985) conducted a doubling CO_2 experiment using coupled full blown atmospheric and oceanic GCMs. However, even with a complicated ocean model the response of the coupled system reflects a fast time scale very much associated with the depth of the mixed layer (in addition to slower time scales involving the deep ocean). So the question about the depth of the upper ocean's mixed layer remains important even in a more realistic model environment.

The last issue is the separation of air–sea heat fluxes into those that force and those that damp the annual cycle in SST. In DH we assumed that SW$\downarrow\uparrow$ is the only forcing and everything else damps. That assumption is certainly in disagreement with Lamb and Bunker's (1982) estimates of SH, LE, LW$\downarrow\uparrow$. Of all these processes, LE has the largest annual cycle and strongly forces SST on account of the undeniable variation in wind speed from summer (weak wind: warming) to winter (strong wind: cooling). The only true damping is LW$\uparrow$ (proportional to T^4) but this aspect is somewhat lost by considering LW$\uparrow\downarrow$ as one process or (even worse) adding LW$\uparrow\downarrow$ with all other terms into the net flux. As far as we can tell, Eq. (6) does not provide an appropriate separation of forcing and damping either, as the ocean transport residual has to be a forcing term in order to explain observed storage. That alone renders Method III somewhat questionable. Until more reliable estimates are available for air–sea exchange as well as ocean transport, Eq. (2)—Method I is apparently the simplest and the best method to calculate h.

Acknowledgments. We thank Charlene Mann for typing the manuscript and Phyllis Stone for her computational assistance. The final version of the manuscript benefitted from the comments made by Dr. S. Hastenrath and an anonymous reviewer. The research was partly supported by NSF Grants ATM-8314431 and ATM-8520877, as well as NOAA Grant NA84-AA-H-00026.

REFERENCES

Bathen, K. H., 1972: On the seasonal changes in the depth of the mixed layer in the North Pacific Ocean. *J. Geophys. Res.*, **77**, 7138–7150.

Bryan, K., and E. Schroeder, 1960: Seasonal heat storage in the North Atlantic Ocean. *J. Meteor.*, **17**, 670–674.

——, and M. J. Spelman, 1985: The ocean's response to a CO_2-induced warming. *J. Geophys. Res.*, **90**, 11 679–11 688.

Bunker, A. F., 1976: Computations of surface energy flux and annual sea–air interaction cycles of the North Atlantic Ocean. *Mon. Wea. Rev.*, **104**, 1122–1140.

——, 1980: Trends of variables and energy fluxes over the Atlantic Ocean from 1948 to 1972. *Mon. Wea. Rev.*, **108**, 720–732.

——, 1988: Surface energy fluxes of the South Atlantic Ocean. *Mon. Wea. Rev.*, **116**, 809–823.

——, and L. V. Worthington, 1976: Energy exchange charts of the North Atlantic Ocean. *Bull. Amer. Meteor. Soc.*, **57**, 670–678.

——, and R. A. Goldsmith, 1979: Archived time-series of Atlantic Ocean meteorological variables and surface fluxes. Woods Hole Oceanographic Institution, Tech. Rep. WHOI 79-3, 27 pp.

Carissimo, B. C., A. H. Oort and T. H. Vonder Haar, 1985: Estimating the meridional energy transport in the atmosphere and ocean. *J. Phys. Oceanogr.*, **15**, 82–91.

Dobson, F. W., and S. D. Smith, 1988: Bulk models of solar radiation at sea. *Quart. J. Roy. Meteor. Soc.*, **114**, 165–182.

Frankignoul, C., and K. Hasselmann, 1977: Stochastic climate models: Part 2: Application to sea-surface temperature anomalies and thermocline variability. *Tellus,* **29,** 289–305.

——, and R. W. Reynolds, 1983: Testing a dynamical model for mid-latitude sea surface temperature anomalies. *J. Phys. Oceanogr.,* **13,** 1131–1145.

Gill, A. E., and P. P. Niiler, 1972: The theory of the seasonal variability in the ocean. *Deep-Sea Res.,* **20,** 141–177.

Hall, M. M., and H. L. Bryden, 1982: Direct estimates and mechanisms of ocean heat transport. *Deep-Sea Res.,* **29,** 339–359.

Hastenrath, S., and P. J. Lamb, 1978: *Heat Budget Atlas of the Tropical Atlantic and Eastern Pacific Ocean.* The University of Wisconsin Press, 104 pp.

——, and J. Merle, 1986: The annual march of heat storage and export in the tropical Atlantic. *J. Phys. Oceanogr.,* **16,** 694–708.

Lamb, P. J., 1984: On the mixed layer climatology of the North and tropical Atlantic. *Tellus,* **36A,** 292–305.

——, and A. F. Bunker, 1982: The annual march of the heat budget of the north and tropical Atlantic Oceans. *J. Phys. Oceanogr.,* **12,** 1388–1410.

Leetmaa, A., and C. S. Welch, 1972: A note on diurnal changes in momentum transfer in the surface layers of the ocean. *J. Phys. Oceanogr.,* **2,** 302–303.

Levitus, S., 1984: Annual cycle of temperature and heat storage in the world ocean. *J. Phys. Oceanogr.,* **14,** 727–746.

——, 1987a: A comparison of the annual cycle of two sea surface temperature climatologies of the world ocean. *J. Phys. Oceanogr.,* **17,** 197–214.

——, 1987b: Rate of change of heat storage of the world ocean. *J. Phys. Oceanogr.,* **17,** 518–528.

Manabe, S., and R. J. Stouffer, 1980: Sensitivity of a global climate model to an increase of CO_2 concentration in the atmosphere. *J. Geophys. Res.,* **85,** 5529–5554.

Meehl, G. A., 1984: A calculation of ocean heat storage and effective ocean surface layer depths for the Northern Hemisphere. *J. Phys. Oceanogr.,* **14,** 1747–1761.

——, and W. M. Washington, 1985: Sea surface temperatures computed by a simple ocean mixed layer coupled to an atmospheric GCM. *J. Phys. Oceanogr.,* **15,** 92–104.

Seckel, G. R., and F. H. Beaudry, 1973: The radiation from sun and sky over the North Pacific Ocean. *Trans. Amer. Geophys. Union,* **54,** 1114.

Simpson, J. J., and C. A. Paulson, 1979: Mid-ocean observations of atmospheric radiation. *Quart. J. Roy. Meteor. Soc.,* **105,** 487–502.

Van den Dool, H. M., and J. D. Horel, 1984: An attempt to estimate the thermal resistance of the upper ocean to climatic change. *J. Atmos. Sci.,* **41,** 1601–1612.

Wilson, C. A., and J. F. B. Mitchell, 1987: A $2 \times CO_2$ climate sensitivity experiment with a global climate model including a simple ocean. *J. Geophys. Res.,* **92,** D11, 13 315–13 343.